Metastability in 2D Self-Assembling Systems

N. V. Medhekar,[1] V. B. Shenoy,[1,*] J. B. Hannon,[2] and R. M. Tromp[2]

[1]*Division of Engineering, Brown University, Providence, Rhode Island 02912, USA*

[2]*IBM Research Division, T. J. Watson Research Center, Yorktown Heights, New York 10598, USA*

(Received 4 June 2007; published 12 October 2007)

We show that 2D self-assembled domains can remain trapped in a large variety of long-lived and metastable shapes that arise from an interplay of crystalline anisotropy and relaxation of elastic strain. On commonly used cubic (111) substrates, these shapes include extended or stacked structures made up of triangular domains connected at their corners, compact shapes with both convex and concave curvatures and others with narrow and elongated arms. We show that all of these distinct experimentally observed shapes can be explained within a unified framework and present a phase diagram that systematically classifies the metastable shapes as a function of their size.

DOI: 10.1103/PhysRevLett.99.156102 PACS numbers: 81.16.Rf, 68.35.Md, 68.43.Hn

The study of shapes of crystals has received considerable attention since the early work of Wulff [1] as it provides quantitative information on the energetics and kinetics of surface processes. Shapes of crystalline nanostructures can also strongly influence their functional (e.g., electrical and optical) properties. According to the classic construction of Wulff [1], the shapes of unstrained crystals in equilibrium are (1) independent of size, (2) always convex, and (3) unique, in the sense that for a given azimuthal dependence of the surface energy, there is a unique shape that minimizes the free energy of the crystal. More recent work has shown that long-range interactions due to elastic, electrostatic, or magnetic effects can complicate this simple picture. In particular, detailed studies of the shapes of 3D crystalline inclusions and quantum dots, 2D surface-stress domains and nanoislands, and epitaxial nanowires have clearly established the size dependence of equilibrium shapes in strained systems.

In case of 2D self-assembling systems, two types of strain-induced shape transitions have been identified: (1) first-order transitions that involve elongation of initially symmetric shapes (squares or circles) along *low-energy* crystalline directions beyond a critical size [2–5] and (2) continuous evolution of stress domains from convex Wulff-like shapes at small sizes to shapes with concave boundaries at large sizes [6]. However, more intriguing shape transitions that do not fall under the two classes described above have also been reported on cubic (111) surfaces widely employed in epitaxial growth. Examples include the connected domain configuration of surface-stress domains on Si(111) [Fig. 1(a)] and elongated shapes of Co islands on Pt(111) with arms that run along *high-energy* crystallographic orientations [Fig. 1(b)] [7].

Motivated by experimental observations of domain shapes on cubic (111) surfaces, we develop a unified description that elucidates and systematically classifies all the possible strain-stabilized shapes in this system. We find that the interplay between elastic relaxation and crystalline anisotropy on these material surfaces gives rise to a large variety of novel shapes not found on their (001) counterparts [2–4]. A key result of this work is the observation that almost all the shapes observed in experiments are not true equilibrium shapes, in the sense of being the *global* minimizers of the total energy, but are configurations trapped in shallow *metastable* minima. Subsequently, for a given size, a unique equilibrium shape will *not* always be obtained in the presence of strain. In what follows, we explicitly map out the energy landscape for strain-induced shapes and present a phase diagram that shows all the possible metastable configurations as a function of the size of the self-assembled domains.

Some of the intriguing shapes of strained domains and islands found on (111) surfaces are given in Fig. 1. Figure 1(a) is an image of an array of (7×7) reconstructed domains on a (1×1) reconstructed Si(111) held in equilibrium at 864 °C. It is well known that difference in surface stress between the two reconstructions ($\Delta\sigma = \sigma_{1\times1} - \sigma_{7\times7}$) plays an important role in the formation and stability of the (7×7) domains [8]. While earlier

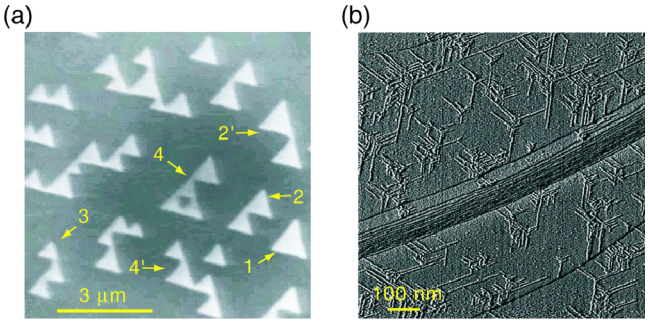

FIG. 1 (color online). (a) LEEM images of (7×7) reconstructed domains on a (1×1) reconstructed Si(111) surface. The domain boundaries are oriented along ⟨110⟩. The areas of the domain marked 1, 2, 2′, 3, 4, 4′ are 0.76, 0.78, 1.33, 0.72, 1.31, and 1.32 μm^2, respectively. (b) STM image of Co islands on Pt(111), with epitaxial mismatch strain of 9% [7]. The three arms of Co islands are 3–5 nm wide and up to 250 nm long. They run *perpendicular* to the close-packed ⟨110⟩ orientations. Reproduced with the permission of the authors [7].

studies [6] have considered the equilibrium shape of isolated compact domains [1 in Fig. 1(a)], other extended shapes with smaller triangular domains connected at their corners [refer to Fig. 1(a)] can also be held without any noticeable change in shape for over 20 min. Furthermore, the sizes of many of these topologically distinct shapes with different numbers of connected triangles are nearly equal. This raises the question as to whether there is a unique "equilibrium" shape for a given domain size. Unlike the domains on Si(111) surfaces, strained Co islands on Pt(111) [7] adopt an entirely different shape. While the domain boundaries in the former case are oriented along the close-packed $\langle 110 \rangle$ directions, highly elongated arms of the Co islands run *perpendicular* to these low-energy orientations. How can we understand these distinct shapes within a unified framework? In what follows, we show that all these shapes are obtained from a simple functional form of the boundary energy as the degree of anisotropy in boundary energy is allowed to vary.

First, we consider the equilibrium shapes of compact domains for the boundary energy, $\beta(\theta) = \beta_0[1 + \alpha(1 - \cos 3\theta)]$, where θ denotes the angle made by the outward normal to the boundary with the horizontal axis and α is the parameter that determines the degree of anisotropy. The total energy of a strained domain can be written as

$$E(A) = \int_s \beta(\theta) ds - \frac{1}{2}\Delta\sigma \int_s \mathbf{n}(s) \cdot \mathbf{u}(s) ds, \qquad (1)$$

where the integrals are taken over the perimeter of the domain, $\Delta\sigma$ is the difference in the surface stresses or the product of the mismatch stress and the height of the islands in the case of coexisting domains or strained monolayer islands, respectively, and $\mathbf{u}$ denotes the elastic displacement fields. Using typical values $\beta_0 = 15.48$ meV/nm, $C_0 = (1 - \nu^2)\Delta\sigma^2/(\pi Y) = 2.853$ meV/nm (where ν is Poisson's ratio and Y is Young's modulus) and an elastic cutoff parameter $\delta = 0.1$ nm [8], we have obtained the equilibrium shapes by minimizing the total energy using a sequential quadratic programming method [9]. The computed shapes for three different values of α are shown in Fig. 2.

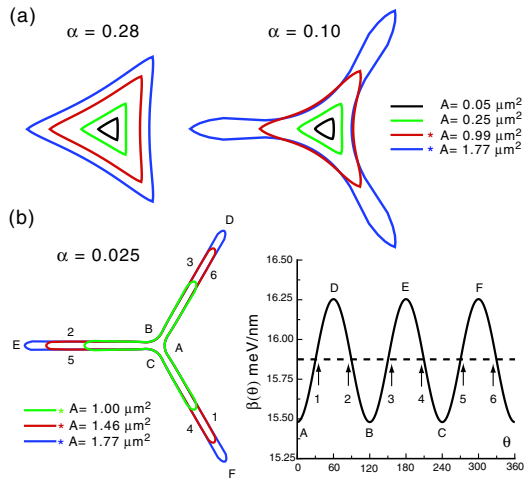

FIG. 2 (color online). Equilibrium shapes of domains on (111) surfaces given for three different values of the anisotropy parameter, α. The domains marked with the * are in metastable equilibrium. The inset in (b) shows the plot of $\beta(\theta)$ with three minima and three maxima labeled A–C and D–F, respectively, and six intermediate orientations labeled 1–6. These orientations are also shown in the equilibrium shapes in (b).

With increasing domain size, the domain boundaries continuously bend towards the center, so that large domain boundaries acquire concave boundaries as reported in Ref. [6]. When the anisotropy becomes smaller, it becomes easier for the boundaries to bend as this leads to efficient relaxation of strain. For the case $\alpha = 0.025$, even at small sizes, the boundaries curve inward to the fullest possible extent until they acquire straight and narrow arms shown in Fig. 2(b). Unlike the shapes for large anisotropy in Fig. 2(a), with increasing size, domains in this case show *shape invariant* growth with constant widths of the side arms. By analytical minimization of the total energy, the width w can be written in a closed form as

$$w = 2a \exp\left(\frac{\alpha\beta_0}{C_0} + \frac{1}{1 - \nu}\right), \qquad (2)$$

where $a = \delta \exp(\beta_0/C_0)$. The widths of the numerically computed shapes in Fig. 2(b) closely agree with this expression.

On a (111) surface the orientations of the six sides of the long arms in Fig. 2(b) correspond to $\langle 112 \rangle$ directions—the boundary energy of these orientations is intermediate between the three low-energy $\langle 110 \rangle$ orientations (A–C) and the other $\langle 110 \rangle$ orientations (D–F) which have the largest boundary energy. The elongated shape therefore involves a significant compromise between the boundary energy (which increases by over 200% relative to the classic Wulff shape) and the relaxation of the elastic energy. This shape predicted by our analysis agrees well with the observed elongation of the arms (that run along $\langle 112 \rangle$) for strained monolayer Co islands on Pt(111) in Fig. 1(b). Since the mismatch strain in this material system is large

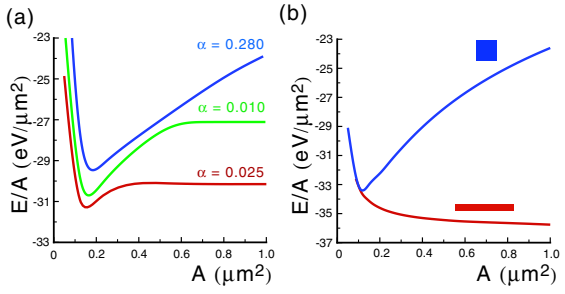

FIG. 3 (color online). Energy per unit area for: (a) domain shapes on a cubic (111) surface given in Fig. 2, and (b) square and rectangular domains on a (001) surface [4]. This quantity attains minimum for the compact domain of size 0.2 μm^2 on the (111) surfaces, while elongated nanowire shape has *smaller* minimum energy per unit area on the (001) surface.

(9.7%), other strain relaxation mechanisms such as defect or dislocation formation have also been observed at very large domain sizes [7]; further quantitative work is needed to obtain the relative importance of the different relaxation mechanisms.

It is evident from Fig. 2 that a wider range of shapes are obtained on (111) surfaces compared to (001) surfaces [2–4]. However, the most significant difference between the two cases relates to the behavior of energy per unit area of the strain-stabilized shapes as plotted in Fig. 3. This quantity is minimum for the infinitely long nanowire shape for (001) surfaces but the minimum is located at a finite size $\approx 0.2\ \mu\text{m}^2$ for domains on (111) surfaces. Since the optimum size is nearly independent of anisotropy in $\beta(\theta)$, it can be estimated using the closed form expression for the total energy of a triangle as

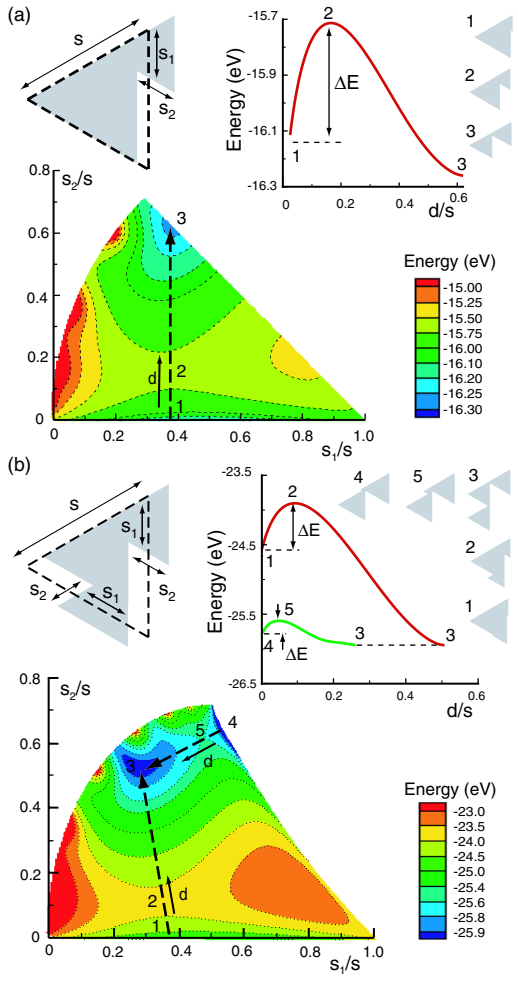

FIG. 4 (color online). Energy landscapes for the growth of notches plotted as a function of their location (s_1) and lengths (s_2): (a) One notch on a domain with area 0.6 μm^2, and (b) Two notches on a domain with area 1.0 μm^2. Insets show the evolution of domain shapes and the corresponding energies along saddle paths. Material parameters used in the calculations, $\beta_0 = 15.48$ meV/nm, $C_0 = 2.853$ meV/nm correspond to the (7×7) domains on Si(111).

$$A_o = a^2 \mu^2 \exp(2), \tag{3}$$

where $\mu = 1.97 \exp[1/(1-\nu)]$. For the parameters used in our analysis $A_o = 0.18\ \mu\text{m}^2$, which is close to the values obtained for all the three cases plotted in Fig. 3. This analysis shows that on (111) surfaces, any domain larger than the optimum size A_o is metastable—the total energy of this domain can be lowered by breaking it up into $N \approx A/A_o$ smaller domains. As we show below, this process however involves a large energy barrier and therefore the shapes marked by the * in Fig. 2 remain trapped in metastable wells. In distinct contrast, the elongated nanowire shape on (001) surfaces corresponds to the global minimum of the total energy.

If an isolated domain has to break up into smaller domains, notches on the boundary have to first nucleate and grow. Here we focus attention on the energy landscapes (Fig. 4) for the growth of notches on straight triangles since the key features apply equally well to domains with curved boundaries. For small domains ($A < 2A_o$), notches never grow as this always leads to an increase in the total energy of the domain. However, for larger domains, it becomes favorable for a notch to grow [Fig. 4(a)], but only after the notch has reached a critical size. In other words, the notch has to overcome a barrier before it can access a new minimum with two connected triangles. The evolution of the domain shapes along the "saddle path" for this case is shown in Fig. 4(a). When the domains become even larger, two notches can grow and lead to a new minimum consisting of three connected triangles as shown in Fig. 4(b). However, the domain in this case can also adopt a *metastable* configuration with two connected triangles. The saddle paths for moving between the different wells in the energy landscape are given in the inset in Fig. 4(b).

Although the total free energy of the connected domains can be further lowered by breaking them into a number of widely *separated* domains of area A_o, the domains in experiments [Fig. 1(a)] as well as in our calculations (Fig. 4) always stay connected at the corners. The strong repulsive elastic interactions between the approaching groove and the straight edge prevents the individual domains from pinching off from the larger connected structure. The equilibrium distance between the V groove and the straight edges obtained from our calculations (50 nm) compares favorably with distances (~20–60 nm) found in experiments. Since repulsive long-range interactions between the approaching boundaries will always prevent pinching, the observed behavior should be generic (for example, see Ref. [10]), but is particularly exaggerated in our experiments because of the small thermal fluctuation amplitudes.

A phase diagram that enumerates the most favorable shapes as a function of the normalized domain size and anisotropy is given in Fig. 5(a). We have obtained this phase diagram by comparing the total energy of shapes with different numbers of notches; this diagram is a gen-

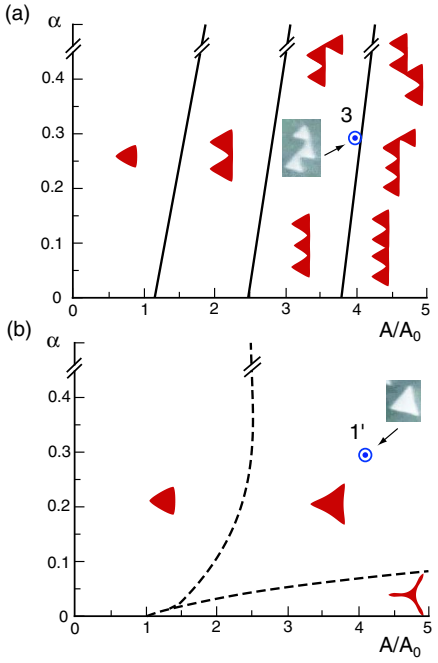

FIG. 5 (color online). Morphological phase diagrams for strained domains on (111) surface as a function of normalized area A/A_o and anisotropy factor α. Part (a) shows optimum connected-domain shapes while part (b) shows the optimum shapes of an isolated compact domain. While energy barriers are encountered in crossing the phase boundaries in (a), the phase boundaries in (b) involve continuous transitions without any barriers. The energy difference between the different shapes with 3 and 4 connected domains is very small (<5%). Points marked 1 and 3 correspond to the Si (7 × 7) domains of nearly identical size in Fig. 1(a). Note that although the total energy of domain 3 is lower, the domain 1 is trapped in a metastable state. The anisotropy parameter for this material system is $\alpha = 0.28$ [11].

eralization of the landscapes in Fig. 4 for shapes with finite anisotropy in $\beta(\theta)$. Also, as in Fig. 4, while the shapes with $N \approx A/A_o$ connected domains is most favorable for a given area, A, other shapes with fewer connected-domains also remain metastable at all sizes. Transitions between the optimal shapes and the metastable shapes involves energy barriers, which are of the order of 0.3–0.7 eV for typical parameters used in our calculations. Clearly, these barriers can never be overcome by thermal fluctuations (<0.12 eV in most experiments). Thus, the final shape adopted by a domain will depend on the number of notches it possessed prior to equilibration. In particular, if there are no notches in the shape, very large isolated domains can remain trapped in metastable shapes given in the phase diagram in Fig. 5(b). Next, we show that these predictions are in agreement with experimental observations on Si(111).

In the case of in Fig. 1(a), the domains were first grown under nonequilibrium conditions that lead to the formation of different number of notches on each domain [11]. The final shapes in Fig. 1(a) were obtained by annealing the nonequilibrium shapes at 864 °C. According to our analysis, during annealing, depending on the number of notches in the initial shape, the domain should evolve to the closest well in the energy landscape and remain trapped there irrespective of its size. This is indeed what is seen in experiment: while the domains marked 1, 2, and 3 in Fig. 1(a) are all of the same size, $A \approx 0.75\ \mu m^2$, they correspond to a compact, two-connected and three-connected shapes, respectively. Similarly for $A \approx 1.3\ \mu m^2$, we find a shape with two connected domains (2′) as well as two shapes with four-connected domains (4 and 4′). These observations are therefore in complete agreement with the energy landscapes and phase diagrams shown in Figs. 4 and 5, respectively.

In summary, we have shown that crystal symmetry plays a very important role in determining the energy landscapes for strained domains. We find significant qualitative differences in the equilibrium shapes on commonly used cubic (001) and (111) surfaces. While the global minimizer in the former case for a given area is a nanowire, in the latter case, it is an array of isolated domains of an optimum size that are widely separated from each other. We have shown here that this configuration is never achieved due to metastability induced by strain. We have presented morphological phase diagrams that predict the size dependence of various metastable shapes that have been observed in experiments. More insights into the interplay between strain and crystalline anisotropy can be gained by extending our analysis to equilibrium shapes on low-symmetry, high-index crystal surfaces.

The research support of the NSF through grant No. CMS-0210095 and the Brown University MRSEC program is gratefully acknowledged.

*Vivek_Shenoy@brown.edu

[1] G. Wulff, Z. Kristallogr. **39**, 449 (1901).
[2] J. Tersoff and R. M. Tromp, Phys. Rev. Lett. **70**, 2782 (1993).
[3] S. H. Brongersma, M. R. Castell, D. D. Perovic, and M. Zinke-Allmang, Phys. Rev. Lett. **80**, 3795 (1998).
[4] A. Li, F. Liu, and M. G. Lagally, Phys. Rev. Lett. **85**, 1922 (2000).
[5] R. van Gastel, N. C. Bartelt, and G. L. Kellogg, Phys. Rev. Lett. **96**, 036106 (2006).
[6] G. E. Thayer, J. B. Hannon, and R. M. Tromp, Nat. Mater. **3**, 95 (2004).
[7] P. Grütter and U. Dürig, Surf. Sci. **337**, 147 (1995).
[8] J. B. Hannon, J. Tersoff, and R. M. Tromp, Science **295**, 299 (2002).
[9] K. Schittkowski, Ann. Oper. Res. **5**, 485 (1986).
[10] R. Plass, N. C. Bartelt, and G. L. Kellogg, J. Phys. Condens. Matter **14**, 4227 (2002).
[11] The formation of notches under nonequilibrium growth conditions has been studied in V. B. Shenoy, N. V. Medhekar, J. B. Hannon, and R. M. Tromp (to be published).